AGU PUBLICATIONS

Paleoceanography

RESEARCH ARTICLE
10.1002/2015PA002787

Key Points:
- Salinity indicates that the process of Agulhas leakage is complex
- We find no evidence of an absence of Agulhas leakage throughout the record
- The ODP Site 1087 record shows an increasing strength of Agulhas leakage

Correspondence to:
B. F. Petrick,
benjamin.petrick@newcastle.ac.uk

Citation:
Petrick, B. F., E. L. McClymont, F. Marret, and M. T. J. van der Meer (2015), Changing surface water conditions for the last 500 ka in the Southeast Atlantic: Implications for variable influences of Agulhas leakage and Benguela upwelling, *Paleoceanography*, *30*, 1153–1167, doi:10.1002/2015PA002787.

Received 4 FEB 2015
Accepted 29 JUL 2015
Accepted article online 1 AUG 2015
Published online 11 SEP 2015

Changing surface water conditions for the last 500 ka in the Southeast Atlantic: Implications for variable influences of Agulhas leakage and Benguela upwelling

Benjamin F. Petrick[1], Erin L. McClymont[2], Fabienne Marret[3], and Marcel T. J. van der Meer[4]

[1]School of Geography, Politics and Sociology, Newcastle University, Newcastle upon Tyne, UK, [2]Department of Geography, Durham University, Durham, UK, [3]School of Environmental Sciences, University of Liverpool, Liverpool, UK, [4]NIOZ Royal Netherlands Institute for Sea Research, Den Burg, Texel, Netherlands

Abstract The Southeast Atlantic Ocean is an important component of global ocean circulation, as it includes heat and salt transfer into the Atlantic through the Agulhas leakage as well as the highly productive Benguela upwelling system. Here we reconstruct sea surface temperatures (SSTs) from Ocean Drilling Program (ODP) Site 1087 in the Southeast Atlantic to investigate surface ocean circulation patterns during the late Pleistocene (0–500 ka). The $U^{K'}_{37}$ index and dinoflagellate cyst assemblages are used to reconstruct SSTs, $\delta D_{alkenone}$ is used to reconstruct changes in sea surface salinity, and mass accumulation rates of alkenones and chlorine pigments are quantified to detect changing marine export productivity. The greatest amplitude of SST warming precedes decreases in benthic $\delta^{18}O$ and therefore occurs early in the transition from glacials to interglacials. The $\delta D_{alkenone}$, as a salinity indicator, increases before SSTs, suggesting that the pattern of Agulhas leakage is more complex than suggested by SST proxies. Marine isotope stage (MIS) 10 shows an anomalous pattern: it is marked by a pronounced increase in chlorine concentration, which may be related to enhanced/expanded Benguela upwelling reaching the core site. We find no evidence of an absence of Agulhas leakage throughout the record, suggesting that there is no Agulhas cutoff even during MIS 10. Finally, the ODP Site 1087 record shows an increasing strength of Agulhas leakage towards the present day, which may have impacted the intensity of the Atlantic meridional overturning circulation. As a result, the new analyses from ODP Site 1087 demonstrate a complex interaction between influences of the Benguela upwelling and the Agulhas leakage through the late Pleistocene, which are inferred here to reflect changing circulation patterns in the Southern Ocean and in the atmosphere.

1. Introduction

The Southeast Atlantic Ocean represents a complex interaction of a number of major oceanic systems, the most important of which are the Agulhas leakage and the Benguela upwelling [*Lutjeharms and Gordon*, 1987; *Boebel et al*., 1999, 2003; *Lutjeharms et al*., 2001; *Knorr and Lohmann*, 2003; *Lutjeharms*, 2007; *Garzoli and Matano*, 2011] (Figure 1). Understanding the history and interaction of these two systems is vitally important to understanding their impact on global climate change. This is because both the Agulhas leakage, which effects the transfer of water from the Indian Ocean to the Atlantic Ocean [*Peeters et al*., 2004; *Martínez-Méndez et al*., 2010; *Beal et al*., 2011; *Caley et al*., 2014], and the Benguela upwelling, which is key for the biological pump [*Andrews and Cram*, 1969; *Andrews and Hutchings*, 1980; *Marlow et al*., 2000; *Rosell-Melé et al*., 2014], have the potential to influence changes in the thermohaline circulation across a range of time scales (Figure 1) [*Bard and Rickaby*, 2009; *Turney and Jones*, 2010; *Beal et al*., 2011].

Several downcore studies have shown that the Agulhas leakage has increased in mass transport and volume over the transitions from glacials to interglacials during the last 410 ka [*Peeters et al*., 2004; *Martínez-Méndez et al*., 2010; *Caley et al*., 2012, 2014; *Marino et al*., 2013]. Since the Agulhas leakage introduces heat and salt to the South Atlantic, these findings have led to the suggestion that the Agulhas leakage could be important in controlling the strength of the Atlantic meridional overturning circulation (AMOC) at the onset and end of interglacials. By increasing the transfer of salt into the Atlantic Ocean, enhanced Agulhas leakage could have strengthened and stabilized the AMOC at the start of interglacials [*Knorr and Lohmann*, 2003; *Peeters et al*., 2004; *Bard and Rickaby*, 2009; *Caley et al*., 2012, 2014]. Based on these findings, it has recently been argued

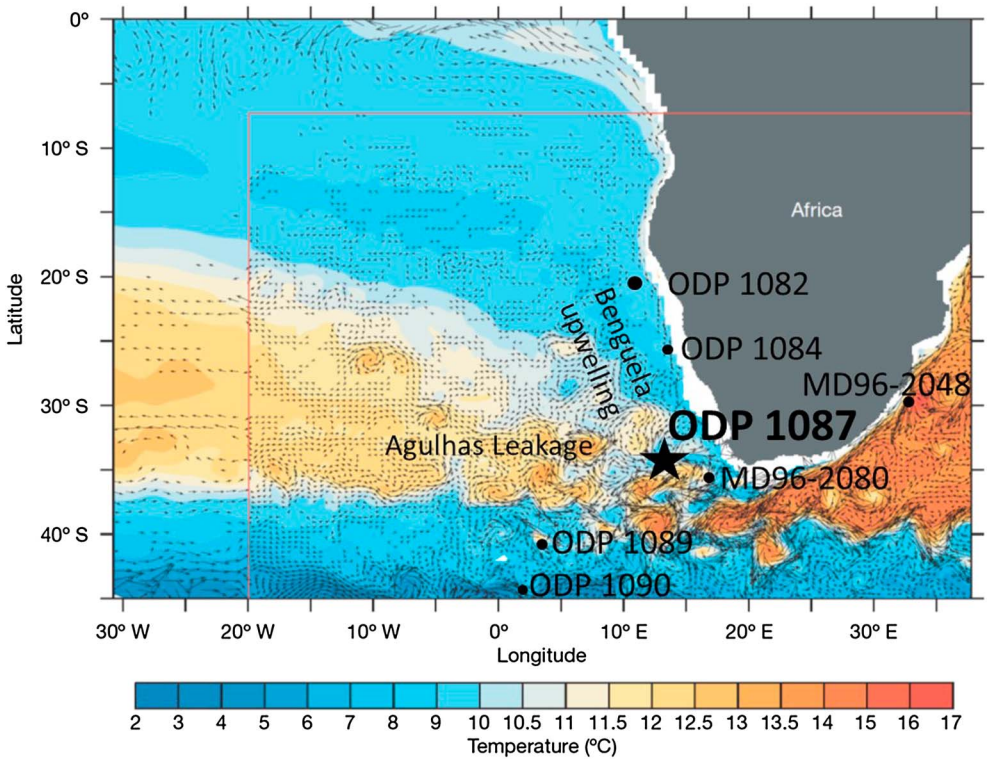

Figure 1. The location of the core site studied here (ODP Site 1087) and other sites discussed in the text, overlain on a map of sea surface temperatures and current strength from *Biastoch et al.* [2008].

that the Agulhas leakage may have been important in the development of "superinterglacials" (warm and/or long interglacials) by increasing the strength of the AMOC (and associated heat transfer) to the northern hemisphere from the southern hemisphere during marine isotopic stages (MISs) 1, 5, 7, and 11 [*Dickson et al*., 2009; *Pollard and DeConto*, 2009; *Masson-Delmotte et al*., 2010; *Turney and Jones*, 2010]. It has also been proposed that any restriction of the Agulhas leakage will lead to a slowdown of AMOC and a weakening of the northward heat transport potential [*Weijer et al*., 1999; *Bard and Rickaby*, 2009; *Beal et al*., 2011]. However, little evidence has been found in existing records of an Agulhas "cutoff." Despite its potential climatic importance, the impact of changes in the Agulhas leakage on global circulation over multiple glacial-interglacial cycles is still not clear.

To the north of the Agulhas leakage lies the highly productive Benguela upwelling system [*Andrews and Hutchings*, 1980]. Decadal resolution alkenone records from the northern part of the upwelling indicate that, with rising global temperatures during the Holocene, the size and intensity of the Benguela upwelling may have increased, in response to the strengthening of the longshore winds and the South Atlantic High pressure cell [*Leduc et al*., 2010]. On the other hand, planktonic foraminiferal assemblages indicate that there were increases in the extent of Benguela upwelling during transitions to glacial periods over the last 400 ka, because a poleward shift in the trade winds during the onset of glaciation allowed more upwelled water to penetrate further offshore from the upwelling region [*Ufkes et al*., 2000; *Ufkes and Kroon*, 2012]. The intensity of upwelling and/or the location of the strongest upwelling in the southern Benguela region are less well known, due to far fewer studies being undertaken. Ocean Drilling Program (ODP) Site 1087 presently lies in the path of Agulhas leakage, but sea surface conditions at the site are expected to be sensitive to any expansion of the upwelling cells of the southern Benguela region [*Giraudeau et al*., 2001].

1.1. Regional Oceanography

The Agulhas Current flows southward along the southeast coast of Africa until the Cape Basin, where it experiences zero stress curl at the point of retroflection [*Lutjeharms*, 2007; *Beal et al*., 2011]. Rings of water are transported northward to the coast of Brazil through geostrophic transport [*Gordon et al*., 1987; *Lutjeharms and Gordon*, 1987]. These "Agulhas rings" are characterized by warmer, saltier water compared

to the surrounding surface ocean. Over time, the heat is dissipated rapidly as the rings are transported north, before then becoming incorporated into the global overturning circulation off the coast of Brazil [*Weijer et al*., 2002; *Boebel et al*., 2003; *Knorr and Lohmann*, 2003; *Lutjeharms*, 2007; *Beal et al*., 2011].

The Benguela upwelling is driven by local longshore winds under the influence of the southeast trade winds, which are in turn controlled by the location and pressure gradient of the South Atlantic High [*Etourneau et al*., 2009; *Hutchings et al*., 2009]. During the austral winter, when the South Atlantic High is far north, very little upwelling occurs in the southern Benguela region (south of 30°) [*Andrews and Hutchings*, 1980; *Hutchings et al*., 2009]. Therefore, the majority of perennial upwelling in the Benguela upwelling takes place in the northern and central parts of the upwelling region [*Andrews and Hutchings*, 1980; *Hutchings et al*., 2009].

1.2. Proxies

To determine the relative importance of Agulhas leakage and southern Benguela upwelling in the Southeast Atlantic over the last 500 ka, we apply a multiproxy approach to reconstruct key oceanographic variables at ODP Site 1087 (Figure 1). We focus on reconstructing sea surface temperatures (SSTs), sea surface salinity (SSS), and export productivity, all key indicators of Agulhas leakage and Benguela upwelling in the modern ocean. SSTs are reconstructed using the $U^{K'}_{37}$ index [*Brassell et al*., 1986; *Prahl and Wakeham*, 1987], which is based on the relative abundance of long-chain C_{37} alkenones with 2 and 3 double bonds synthesized by a few species of haptophyte algae [*Volkman et al*., 1980; *Brassell et al*., 1986; *Prahl et al*., 1988]. The alkenone distribution has been shown to vary with temperature in cultures, water column, and sediment samples [*Brassell et al*., 1986; *Prahl and Wakeham*, 1987; *Prahl et al*., 1989; *Müller et al*., 1997; *Conte et al*., 2006]. We also investigated changes to dinoflagellate assemblages, which are microscopic unicellular organisms that produce tests of organic material (dinocysts) that can be preserved in sediments. Dinoflagellates have certain ecological or environmental niches that can be determined in the paleorecord [*Zonneveld et al*., 2001; *Marret and Zonneveld*, 2003; *De Schepper et al*., 2009] and have successfully been used for reconstructing sea surface conditions [*de Vernal and Hillaire-Marcel*, 2000; *de Vernal et al*., 2005]. We used compound-specific deuterium/hydrogen isotope ratios of the C_{37} alkenones as an indicator for changes in SSS [*Schouten et al*., 2006; *Van der Meer et al*., 2007, 2013; *Kasper et al*., 2014; *M'boule et al*., 2014]. This method has recently been applied to reconstruct SSS changes associated with Agulhas leakage in the Southeast Atlantic Ocean, to the south of ODP Site 1087, over the last two glacial-interglacial transitions [*Kasper et al*., 2014]. One advantage of using the alkenones to reconstruct SST, SSS, and alkenone mass accumulation rates (MARs) as indicator for productivity (see below) is that these signals are being recorded by the same proxy carrier, reducing errors associated with transport (timing), species, and habitat differences.

Export production is reconstructed using the concentrations of the chlorine pigments and the C_{37} and C_{38} alkenones. Chlorines are the sedimentary products of the photosynthetic pigment chlorophyll and are considered to represent changes in export productivity, given the positive relationship between concentrations of chlorophyll *a* in the surface ocean and associated chlorine concentrations in the underlying surface sediments [*Harris et al*., 1996; *Szymczak-Zyla et al*., 2011]. However, quantitative reconstructions of export production are limited by the additional influences of organic matter degradation, which occur during and after transport to the sediment record [*Szymczak-Zyla et al*., 2011]. Additionally, variable sedimentation rates and dilution also affect these data. Alkenone concentrations have been shown to reflect export primary production changes at ODP Site 1087, giving good correspondence between the accumulation rates of alkenones and coccoliths and spring upwelling [*McClymont et al*., 2005; *Lee et al*., 2008]. Here we interpret the chlorine and alkenone accumulation rate data as qualitative indicators of past export productivity.

2. Methods

2.1. Sampling and Age Model

For ODP Site 1087A (31°28′S, 15°19′E; 1374 m water depth; Figure 1) the age model was updated by retuning the benthic $\delta^{18}O$ record to the LR04 benthic stack [*Lisiecki and Raymo*, 2005], by matching significant peaks in both records to achieve the best correlation (highest R^2) using the computer program AnalySeries [*Paillard et al*., 1996]. The maximum offset between the old and new age models for the site is 10 ka. The mean sampling resolution presented here (4 cm) is equivalent to 4 ka.

2.2. Alkenone and Chlorine Extraction and Quantification

Freeze-dried and homogenized samples were solvent extracted using a CEM MARS 5 microwave system and following the methodology of *Kornilova and Rosell-Mele* [2003]. Around 3.5 g of sediment was extracted with 12 mL of dichloromethane (DCM): methanol (3:1) by heating to 70°C for 5 min, holding at 70°C for 5 min, and allowing the sample to cool. Extracts were recovered by centrifugation. The supernatant was transferred to a clean preweighted sample vial and dried under a stream of nitrogen to obtain a total lipid extract. A fraction of the total extract was analyzed for alkenones, by first derivatizing the total lipid extract using N_2O-Bis(trimethlsiyl)trifluoroacetamide with trimethylchorosilane and heating to 70°C for 1 h. The alkenone aliquots were analyzed using a gas chromatography (GC) fitted with a flame ionization detector and a 30 m HP1-MS capillary column. Hydrogen was the carrier gas (3 mL min^{-1}, column head pressure 124,110 Pa). The injector temperature was held at 300°C and the detector at 310°C. After injection, oven temperature was held at 60°C for 1 min, then increased at 20°C/min to 120°C, to 310°C at 6°C m^{-1}, and held at 310°C for 30 min. Alkenone identification was confirmed through analysis by GC–mass spectrometer. The peak areas of the C_{37} alkenones with two and three unsaturations were used to calculate the $U^{K'}_{37}$ index and converted into SST values using the sediment core top calibration of *Müller et al*. [1998]. The proxy has a calibration and reproducibility error of 1.1°C within 2 standard deviations [*Conte et al*., 2006].

Total chlorine concentrations were measured on a separate lipid extract aliquot by UV/visible light spectrometer (VIS) spectrophotometry. The chlorine aliquot was dissolved in 2 mL acetone, transferred to a quartz cuvette and analyzed by a WPA Lightwave UV/VIS diode array spectrophotometer. Triplicate readings were taken at 410 nm and 665 nm wavelengths, which correspond to the principal absorbance of chlorophyll pigments [*Rosell-Melé et al*., 1997]. Chlorines were quantified as absorbance per gram of dry weight extracted sediment (abs g^{-1}) and then converted to MAR using our new linear sedimentation rates and the shipboard dry bulk density measurements [*Shipboard Scientific Party*, 1998] following the approach of *Emeis et al*. [1995].

2.3. Alkenone δD Analysis

Fifty alkenone samples were selected for compound specific isotope analysis. Selection was guided by the SST record, in order to cover transitions to and from interglacial maxima. Our sampling strategy also ensures comparison to the existing data for two deglaciations from a site to the south [*Kasper et al*., 2014]. The total lipid extract was separated over an Al_2O_3 column into an apolar, ketone, and polar fractions using hexane: DCM 9:1, hexane:DCM 1:1, and DCM:methanol 1:1 (vol/vol), respectively. Alkenone fractions were checked for purity and concentration by GC [*Kasper et al*., 2015].

Alkenone hydrogen isotope analyses were carried out on a Thermo Scientific DELTA$^+$ XL GC/thermal conversion/isotope ratio mass spectrometry. The temperature conditions of the GC increased from 70 to 145°C at 20°C min^{-1}, then at 8°C min^{-1} to 200°C and to 320°C at 4°C min^{-1}, at which it was held isothermal for 13 min using an Agilent CP-Sil 5 column (25 m × 0.32 mm) with a film thickness of 0.4 μm and helium as carrier gas at 1 mL min^{-1} (constant flow). The high-temperature conversion reactor was set at a temperature of 1425°C. The H_3^+ correction factor was determined daily and was constant at 4.7 ± 0.1 for the first batch of samples and 5.6 ± 0.25 for the majority of the samples. A set of standard *n*-alkanes with known isotopic composition (Mixture B prepared by Arndt Schimmelmann, University of Indiana) was analyzed daily prior to analyzing samples in order to monitor the system performance. Samples were only analyzed when the alkanes in Mix B had an average deviation from their off-line determined value of <5‰. Squalane was coinjected as an internal standard with each sample to monitor the accuracy of the alkenone isotope values. The squalane standard yielded an average $\delta D_{alkenone}$ value of −166‰ ± 2.4, which compared reasonably well with its off-line determined δD value of −170‰. The $\delta D_{alkenone}$ values were measured as the combined peak of the $C_{37:2}$ and $C_{37:3}$ alkenones ($\delta D_{alkenone}$) [*Van der Meer et al*., 2013].

2.4. Dinoflagellate Analysis

Seven freeze-dried samples were analyzed for dinoflagellate cyst assemblages, following the method described in *Marret et al*. [2008]. Dry sediment samples were weighed, and their volume was estimated. Prior to the treatment of samples, a tablet of exotic markers (*Lycopodium clavatum*) was added to each sample to assess the concentrations of palynomorphs. The sediments were digested using the addition of cold 10% hydrochloric acid to decalcify the samples. This preparation was followed by adding cold 40% hydrofluoric acid to remove the siliceous fraction. Finally, a third rinse of cold 10% hydrochloric acid removed

any remaining calcite. The digested samples were passed through a 10 μm sieve to remove fine fraction sediments. The residue was mounted on glass slides and then investigated under a microscope. A minimum of 100 specimens were counted per sample to give a statistically significant number [*Marret et al.*, 2008]. Sea surface temperatures were estimated using the dinoflagellate cyst reconstruction based on the modern analogue technique. The modern data set comprises 208 sites and was presented in *Marret et al.* [2008]; surface conditions were extracted from the World Ocean Atlas 2001 [*Conkright et al.*, 2002]. The calibration of the modern data set yields an accuracy of ±1.23°C within 2 standard deviations for annual SST.

3. Results

3.1. $U^{K'}_{37}$ SSTs

Overall, the $U^{K'}_{37}$ values range from 0.4 to 0.8 units (15 to 21°C) on glacial-interglacial time scales over the past 500 ka (Figure 2a). Recent research in the use of temperature proxies in the Benguela upwelling showed that $U^{K'}_{37}$ values were the least affected by outside forcings such as the amount of upwelling and seasonality [*Lee et al.*, 2008]. A pronounced cool interval is recorded at 375 to 350 ka (MIS 10), where SSTs fall to 12°C. The highest SSTs are recorded around 243 to 228 ka and 135 to 112 ka (MISs 7 and 5). A comparison with the benthic δ^{18}O record for ODP Site 1087 (Figure 2e) shows that, even with the 4–3 ka sampling resolution presented here, suborbital-scale warming trends in $U^{K'}_{37}$ precede all interglacial onsets as defined by *Lisiecki and Raymo* [2005] The deglacial warming leads major decreases in benthic δ^{18}O by 4–10 ka on average during transitions, with the earliest onset of warming identified ~30 ka before the start of MIS 1. During the transition to MIS 11, SSTs peak at 20°C, approximately 5 ka before the onset of the interglacial as defined by benthic δ^{18}O, whereas the interglacial maximum, as defined by benthic δ^{18}O, has lower SSTs than during the deglaciation (18.5°C at ~403 ka). Finally, there is a warming trend of the interglacial maxima over the last 500 ka and an overall warming trend in the glacial minima since 300 ka.

3.2. Alkenone δD

The $\delta D_{alkenone}$ isotope values range from a minimum of −213‰ to a maximum of −179‰, and the average value over the entire record is −196‰ (Figure 2b). The glacial-interglacial $\delta D_{alkenone}$ alkenone shifts are larger than expected based on the benthic δ^{18}O shift, suggesting that it cannot be explained by only an ice volume effect [*Kasper et al.*, 2014, 2015]. Furthermore, the lack of correlation between the $\delta D_{alkenone}$ and the alkenone MAR excludes growth factors as major contributors to changes in the hydrogen isotopic composition of alkenones (Figure 2) [*Schouten et al.*, 2006; *Kasper et al.*, 2014, 2015]. Lastly, there is no evidence in the alkenone distributions that would suggest significant species change [*McClymont et al.*, 2005], which could also have affected the $\delta D_{alkenone}$ [*Schouten et al.*, 2006; *Chivall et al.*, 2014; *Kasper et al.*, 2014, 2015; *M'boule et al.*, 2014]. Therefore, it is likely that the $\delta D_{alkenone}$ values represent changes in SSS [*Kasper et al.*, 2014, 2015; *M'boule et al.*, 2014].

The $\delta D_{alkenone}$ shows a consistent pattern over multiple glacial-interglacial transitions, with large decreases (20‰) in $\delta D_{alkenone}$ occurring during the deglaciations and positive values before the deglaciation as defined by δ^{18}O. The largest decrease (−215‰) in $\delta D_{alkenone}$ occurs at MIS 12/11. The longer-term trend in $\delta D_{alkenone}$ is increasing values toward the present, such that the highest $\delta D_{alkenone}$ values are recorded during MIS 2 (Figure 2b).

3.3. Dinoflagellate Cyst Assemblage SSTs

Seven samples were selected for dinocyst SST analysis (Figure 2a), in order to compare evidence of leakage/upwelling with alkenone-derived SSTs. Overall, the dinoflagellate cyst assemblage diversity is relatively small, with only 13 species identified. The assemblages are mostly dominated by *Operculodinium centrocarpum* and *Nematosphaeropsis labyrinthus* and have significant percentages of *Spiniferites ramosus*. *Operculodinium centrocarpum* is a cosmopolitan species that thrives in unstable conditions, whereas *N. labyrinthus* is more restricted to open oceanic conditions. *Spiniferites ramosus* is a subpolar to subtropical species and is often abundant in upwelling regions [*Marret and Zonneveld*, 2003; *Marret et al.*, 2008]. SSTs were estimated and show values between 17 and 18.5°C (Figure 2a). Sea surface temperature estimates from dinoflagellate cyst assemblages are in broad agreement with the SSTs reconstructed using alkenones throughout the interval (Figure 2a).

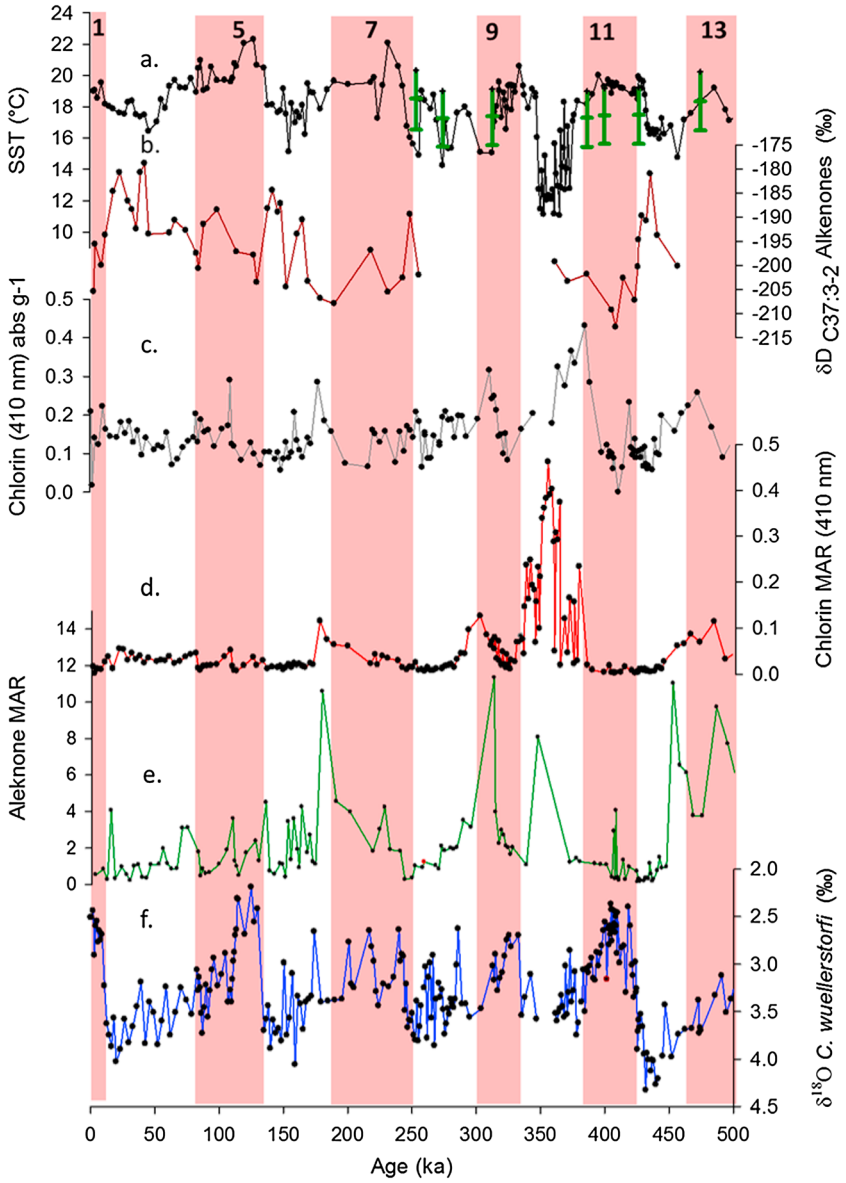

Figure 2. New late Pleistocene records of SST, salinity, and pigments from ODP Site 1087. The red bars represent the interglacials delineated according to the LR04 stratigraphy [*Lisiecki and Raymo*, 2005], and marine isotope stage (MIS) numbers are marked. (a) U^{K}_{37}' SST record (black) calculated using the calibration of *Müller et al.* [1998] and SST range (summer to winter temperature range) calculated using dinoflagellate assemblages (green) estimated according to *Marret et al.* [2008]. (b) Record of $C_{37:2\text{-}3}$ alkenone δD representing changes in salinity. (c) Chlorine concentration record (absorbance at 410 nm). (d) Chlorine mass accumulation rate (MAR) abs (kyr cm^2)$^{-1}$ record (absorbance at 410 nm). (e) Alknone mass accumulation rate (MAR) µg (kyr cm^2)$^{-1}$ record. (f) Record of benthic δ^{18}O from *C. wuellerstorfi* [*Pierre et al.*, 2001], retuned to the LR04 global benthic δ^{18}O stack [*Lisiecki and Raymo*, 2007] after *McClymont et al.* [2005].

3.4. Chlorine and Alkenone Accumulation Rates

Chlorine concentrations range from 0.05 to 0.48 g^{-1} (Figure 2c). Broad peaks in chlorine concentrations occur at 486 ka, 350 ka, 304 ka, and 179 ka. The amplitude of the chlorine peaks diminishes in intensity and duration during interglacials, from a maximum at MIS 10 to a minimum during MIS 3. During MIS 10 the pronounced and extended chlorine concentration maxima (0.3–0.4 g^{-1} over ~50 ka) corresponds to the minimum in SSTs recorded in the alkenones (Figure 2a). When changes in sediment mass accumulation rates (MARs) are taken into account, the unusually high chlorine content of MIS 10 is further emphasized: chlorine MAR during MIS 10 is around 0.50 (cm^2 kyr^{-1})$^{-1}$ MAR (Figure 2d). Additional minor increases in chlorine MAR occur at 486 ka,

304 ka, and 179 ka (all with similar values of 0.1 $(cm^2\,kyr^{-1})^{-1}$. No long-term trend in chlorine concentration or chlorine MAR is detected over the last 500 ka.

The alkenone MAR values range from 11.3 μg $(abs\,cm^2\,kyr^{-1})^{-1}$ to 0.1 μg $(abs\,cm^2\,kyr^{-1})^{-1}$. In general, alkenone MAR values are higher during glacial periods and lower during interglacials, with maxima recorded during MIS 12 and minima during MIS 11 and MIS 1.

4. Discussion

4.1. Early Deglacial Warmings and Salinity Increases Over the Past 0.5 Ma

The late Pleistocene $U^{K'}_{37}$-SST record from ODP Site 1087 is marked by a series of warming events which precede the onsets of the deglacial decreases in $\delta^{18}O$ by 4 ka to 10 ka, supported by the dinocyst-based SSTs (Figures 2a and 2e). Furthermore, increases in SSS ($\delta D_{alkenone}$) lead the onset of sea surface warming at this site by 4–8 ka and therefore begin approximately 8–18 ka before the onset of the interglacials. As SSTs rise, SSS decreases and then remains relatively low throughout the duration of interglacials (Figure 2). Therefore, for the last 500 ka in the ODP Site 1087 record, there is evidence that the onset of interglacials is marked by a $\delta D_{alkenone}$ or SSS maximum followed by a rise in SSTs.

In the modern ocean, the signature of Agulhas rings (and thus, leakage) is an increase in sea surface temperature and salinity relative to the Atlantic or Benguela upwelling waters, given the properties of their source, the Agulhas Current (Figure 1) [*Lutjeharms and Gordon*, 1987; *Lutjeharms*, 1994, 2007; *Penven et al*., 2001]. Therefore, the most likely source for warmer and higher-salinity water to ODP Site 1087 is an increased contribution from the Agulhas leakage, which we infer to have occurred during every deglaciation for the last 500 ka. Early localized warming and/or increased inputs of Agulhas leakage fauna preceding interglacial maxima have been identified previously in the Southeast Atlantic during the late Pleistocene [*Peeters et al*., 2004; *Martínez-Méndez et al*., 2008; *Dickson et al*., 2010; *Marino et al*., 2013; *Caley et al*., 2014]. Figure 3 shows a comparison of SST reconstructions from other cores in the region, including MD96-2048, MD96-2080, ODP Site 1082, ODP Site 1089, and ODP Site 1090 (locations shown in Figure 1). The early deglacial warmings at ODP Site 1087 are also observed in cores MD96-2080 and MD96-2048 [*Martínez-Méndez et al*., 2008, 2010], which are situated within the origin of Agulhas leakage within the uncertainty introduced by the differences in age models and sampling resolutions (MD96-2080 is based on both $\delta^{18}O$ and C^{14} dating, which means that there is an error of about <1 ka for the last deglaciation and about 4–5 ka after that). Therefore, early deglacial warmings are synchronous between sites [*Martínez-Méndez et al*., 2008, 2010]. This is further evidence that the warming trends at ODP Site 1087 likely reflect changing conditions upstream in the Agulhas retroflection.

Caley et al. [2012] observed enhanced accumulations of the subtropical planktonic foraminiferal species *Globorotalia menardii* for every deglaciation during the last 500 ka at ODP Site 1087 (Figure 3), as also observed by *Peeters et al*. [2004] at a site closer to the Agulhas retroflection. Since *G. menardii* is specific to warm waters, and during glacial periods is restricted to the Indian Ocean [*Peeters et al*., 2004; *Caley et al*., 2012, 2014], its presence in ODP Site 1087 was suggested to reflect early "reseeding" events during deglaciations as a result of the Agulhas leakage [*Rau et al*., 2002; *Caley et al*., 2012]. However, other studies suggest that the presence or absence of *G. menardii* in the Atlantic Ocean is controlled by the ventilation of the thermocline [*Sexton and Norris*, 2011]. A change in low-latitude ventilation in intermediate water bodies during the glacial period is hypothesized to reduce the number *G. menardii* in the Atlantic Ocean by changing the oxygen content of the thermocline [*Sexton and Norris*, 2011]. This raises questions about whether the pattern seen in the record is a result of changes in oxygen minima or a result of Agulhas leakage. More recent work has estimated Agulhas leakage using a range of Indian Ocean foraminifera at ODP Site 1087 to create an index to estimate leakages [*Caley et al*., 2014]. This index shows a similar pattern at ODP Site 1087 as the *G. menardii* data [*Caley et al*., 2014]. Therefore, it seems that at ODP Site 1087 the *G. menardii* data are influenced at least in part by Agulhas leakage. However, more work is necessary to confirm these patterns seen in the record and to understand the effect of oxygen changes.

Despite the similar timings between increasing volume of leakage and increasing temperatures, there seems to be a decoupling in the timing of inputs of SSTs and SSS at ODP Site 1087 according to the $\delta D_{alkenone}$. The earlier increases at ODP Site 1087 in SSS challenge the straightforward interpretation of SST warming equalling enhanced leakage (and assumed enhanced salt transfer). Increases in SSS as indicated by $\delta D_{alkenone}$

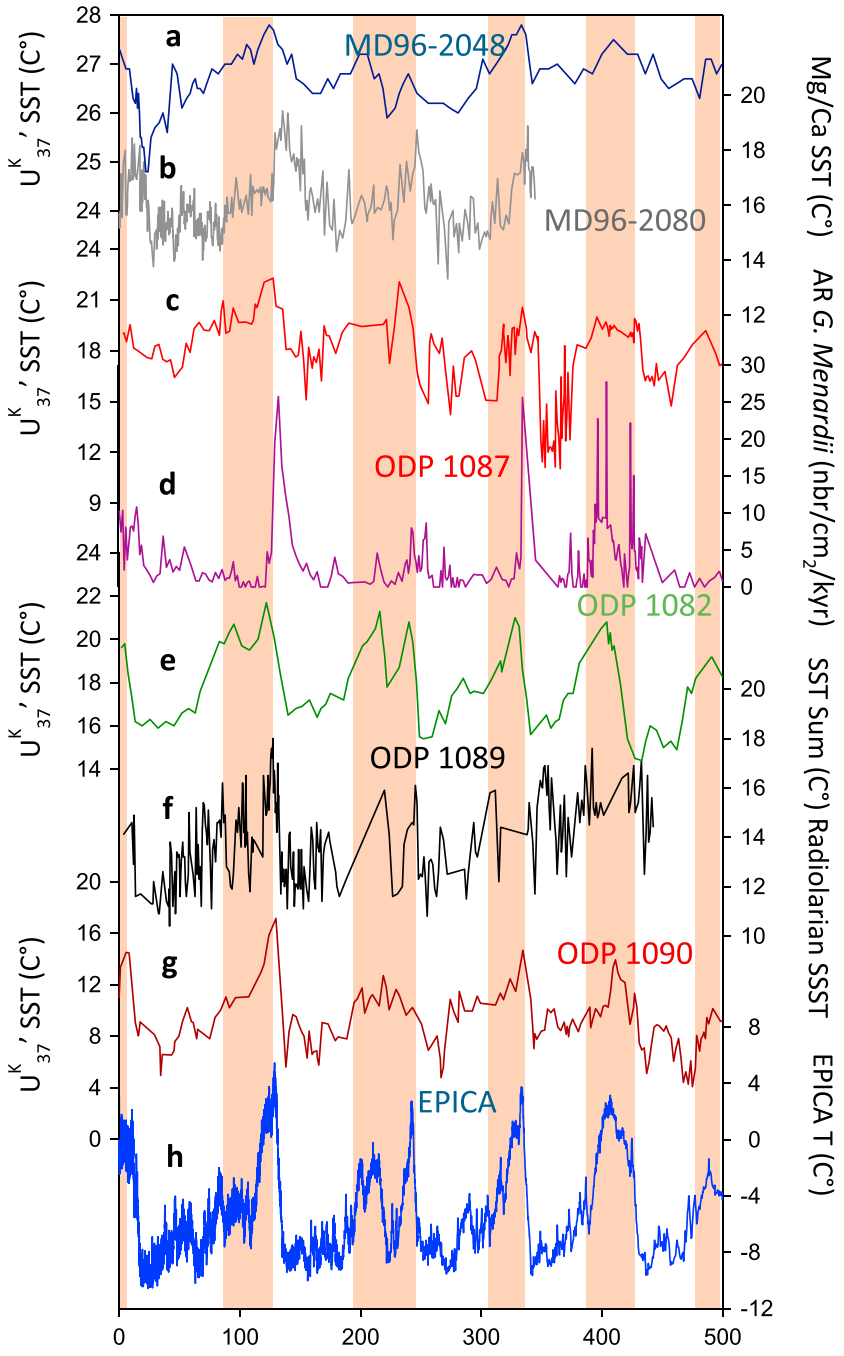

Figure 3. SST records from the Agulhas Current and Agulhas leakage region. Site locations are shown in Figure 1. Most of these age models are based on benthic δ^{18}O records that have been correlated to other benthic δ^{18}O records or LR04 with the exception of ODP 1089 [*Cortese and Abelmann*, 2002]. (a) M96-2048 U^{K}_{37}′ SST from the Indian Ocean, upstream in the Agulhas Current [*Caley et al.*, 2011]. (b) Agulhas Bank Mg/Ca SST from the leakage origin zone [*Martínez-Méndez et al.*, 2008]. (c) ODP Site 1082 U^{K}_{37}′ SST record from the Benguela upwelling [*Etourneau et al.*, 2009]. (d) ODP Site 1087 U^{K}_{37}′ SST (this study). (e) ODP Site 1087 *G. menardii* concentrations [*Caley et al.*, 2012]. (f) ODP 1089 radiolarian-based temperatures, from just north of the Antarctic Circumpolar Current (ACC) [*Cortese and Abelmann*, 2002]. (g) ODP 1090 U^{K}_{37}′ SST from the sub-Antarctic zone of the ACC [*Alonso-Garcia et al.*, 2011]. (h) Antarctic δD record of air temperature [*European Project for Ice Coring in Antarctica*, 2004]. The blue bars represent the glacial periods.

before SST during deglaciations have also been observed in sites MD96-2080 and MD02-2594, to the south of ODP Site 1087 [*Kasper et al*., 2014]. A salinity maximum occurred during the terminations and early interglacials at Walvis Ridge at thermohaline depths [*Scussolini et al*., 2015]. If both of these records are reflecting Agulhas leakage it might indicate that the salinity recorded in ODP Site 1087 core is reflecting a different transport pathway than at Walvis Ridge. This suggests that the depth of maximum salinity leakage increases as the volume of the leakage increases.

Kasper et al. [2014] proposed that the $\delta D_{alkenone}$ pattern reflected salinity buildup in the southern Indian Ocean during the glacial period when there was weaker Agulhas leakage, followed by a release of high-salinity waters into the Atlantic during the initial increase in Agulhas leakage during deglaciations [*Kasper et al*., 2014]. Our new data from ODP Site 1087 show (1) that this pattern is sustained over multiple deglaciations of the last 500 ka, including the transitions at MIS 6/7 and MIS 10/11, and (2) that there are long-term trends in both SST and SSS as indicated by $\delta D_{alkenone}$ since 500 ka (Figure 2) [*Peeters et al*., 2004; *Martínez-Méndez et al*., 2010].

4.2. Potential Controls Over Agulhas Leakage

MIS 10 is unusual in our record, since it is marked by sustained low SSTs and high-chlorine MAR (Figure 2). Additionally, there is a change in the dominant species in the dinocysts at the end of MIS 11 from *O. centrocarpum* to *N. labyrinthus*. *O. centrocarpum* is well known to currently be dominant in waters at the edge of the Benguela upwelling, while *N. labyrinthus* is found in higher-nutrient environments [*Marret and Zonneveld*, 2003]. This suggests a shift in the dominant environment of the core site from the edge of the upwelling to a more nutrient-rich site, which is likely more influenced by upwelling waters. It is possible that increasing amounts of winter mixing could be responsible for this pattern as well [*Lee et al*., 2008]. However, if we assume that alkenone production during MIS 10 was similar to the present [*Lee et al*., 2008], the high concentrations of alkenones would suggest higher production during spring [*Lee et al*., 2008]. It cannot be definitively proven what process is affecting the high productivity at the site. However, given our current understanding on the South Atlantic oceanic and atmospheric circulation links, the balance of the evidence points to source water from the upwelling zone reaching ODP Site 1087 [*Petrick et al*., 2015]. MIS 10 was also identified as a particularly cold glacial stage in a site close to (but not in) the Agulhas Current [*Bard and Rickaby*, 2009] (MD96-2077), whereas the lack of major cooling within the Agulhas Current [*Caley et al*., 2011] (MD96-2048) argues against an upstream control over SSTs at ODP Site 1087 (Figure 3). In contrast, at ODP Site 1089 (to the south of ODP Site 1087) MIS 10 is marked by relatively warm SSTs (Figure 3) [*Cortese et al*., 2004, 2007]. Since ODP Site 1089 lies just south of the normal path of the Agulhas leakage, the warmth of MIS 10 has been interpreted to reflect an increase in the intensity of Agulhas leakage during this glacial period [*Cortese et al*., 2004]. The cooler SSTs at ODP Site 1087 (but warmth at ODP Site 1089) during MIS 10 could be explained by a southward shift in the main zone of Agulhas leakage. This hypothesis requires further testing using analysis of Agulhas leakage fauna and evidence for SSS (e.g., by $\delta D_{alkenone}$) at ODP Site 1089 but suggests that during MIS 10 there was a displacement, rather than a cutoff of Agulhas leakage to the Southeast Atlantic.

To account for the pronounced cooling and enhanced export production at ODP Site 1087 during MIS 10, we infer that expansion of upwelling sourced water occurred in the southern Benguela region. This interpretation is supported by evidence from planktonic foraminiferal assemblages from the Walvis Ridge, which were interpreted to reflect upwelling expansion at ~400 and 325 ka [*Ufkes et al*., 2000; *Ufkes and Kroon*, 2012]. ODP Site 1084, in the central Benguela region and under the main upwelling cell at present, also shows strong cooling during MIS 8 and MIS 10 [*Rosell-Melé et al*., 2014]. Foraminiferal reconstructions from ODP Site 1087 found the presence of upwelling waters in the record at the start of MIS 9 [*Giraudeau et al*., 2001], the only time in the last 500 ka that foraminifera indicating active upwelling were observed at ODP Site 1087 [*Giraudeau et al*., 2001].

Finally, the biogeochemical data indicate MAR values similar to the late Pliocene when upwelling water is believed to have affected this site [*Petrick et al*., 2015].

Both the Agulhas leakage and Benguela upwelling systems are linked to the regional wind fields, which include the westerlies, trade winds, and local winds. It has been shown that the currents around southern Africa might be susceptible to changes in the global wind field [*de Ruijter and Boudra*, 1985; *Boudra and De Ruijter*, 1986;

Olson and Evans, 1986; *Franzese et al*., 2006a; *Kohfeld et al*., 2013]. At the same time as the long-term warming trend (and inferred intensification of Agulhas leakage) at ODP Site 1087 over the last 500 ka, dust proxies show that the westerlies have also intensified and shifted in the Southern Ocean [*Martinez-Garcia et al*., 2011]. The strengthening and southward shift of the westerlies and the weakening and northward movement of the Hadley cells strengthen the amount of leakage by shifting the location of the Subtropical Front southward and in turn opening up the ocean to the south of the African continent [*Biastoch et al*., 2009; *Beal et al*., 2011; *De Deckker et al*., 2012]. Conversely, the strengthening of the Hadley cells and northward movement of the westerlies during the glacials may block or restrict the Agulhas leakage while also extending the geographical reach of Benguela sourced water during glacials. As a wind-driven system, the cause of the expanded upwelling sourced water during MIS 10 most likely relates to intensification and/or southward displacements of the Hadley cells, allowing upwelled waters to expand outward away from their normal extent [*Ufkes et al*., 2000; *Ufkes and Kroon*, 2012]. It is also important to note that modeling studies show that the local wind fields in the Southeast Atlantic are complex, making it hard to identify specifically whether shifts in the trade winds, westerlies, or local coastal wind changes can cause a change to the Agulhas leakage position and strength [*De Boer et al*., 2013; *Kohfeld et al*., 2013]. Further work is required to examine the interaction between the regional winds, Agulhas leakage, and upwelling extent and intensity on the orbital time scales presented here.

4.3. Late Pleistocene Superinterglacials

A number of authors have argued that increased Agulhas leakage caused the strengthening of the AMOC at the start of the last interglacial [*Peeters et al*., 2004; *Caley et al*., 2012, 2014]. It has even been suggested that increased Agulhas leakage at the start of an interglacial may be responsible for superinterglacials [*Turney and Jones*, 2010]. There is no current consensus on what a superinterglacial is. MISs 1, 5, 9, and 11 have all been described as superinterglacials, given their duration and/or temperature signal [*Berger and Loutre*, 2002; *Loutre and Berger*, 2003; *de Abreu et al*., 2005; *DeConto et al*., 2007; *Turney and Jones*, 2010; *Turney et al*., 2011]. There is some evidence at ODP Site 1087 to support the proposed connection between more Agulhas leakage and longer and warmer superinterglacials. The superinterglacials of MISs 1, 5, 9, and 11 are marked by deglacial warming, and Agulhas leakage increases at ODP Site 1087 based on SSTs and $\delta D_{alkenone}$ records (Figure 2), suggesting a strong input of predeglaciation Agulhas leakage.

Other parts of our record, however, raise questions about the superinterglacial theory. MIS 7 is the only interglacial of the last 500 ka that has not been identified as a superinterglacial [*DeConto et al*., 2007]. At ODP Site 1087, it has some of the warmest SSTs in the last 500 ka, suggesting that locally there was an input of warm water compared to the rest of the Southeast Atlantic, which is inferred here to indicate some influence of Agulhas leakage during MIS 7 (Figure 2), yet it did not result in a superinterglacial. Another proposed superinterglacial is MIS 11, which is argued to be one of the most prominent and warm interglacials globally [*Loutre and Berger*, 2003; *de Abreu et al*., 2005; *Pelejero et al*., 2006; *Dickson et al*., 2009]. Recent research has suggested that increased Agulhas leakage at the end of MIS 11 might have extended the interglacial [*Dickson et al*., 2009, 2010; *Koutsodendris et al*., 2014]. However, at ODP Site 1087, the SSTs are slightly cooler during MIS 11 than during almost all of the other interglacials over the last 500 ka, suggesting a reduced influence of Agulhas leakage.

In contrast to the complex SST signal, there is a better correlation between SSS and the length of interglacials. Because MIS 11 is similar to MIS 1 in terms of length, and orbital configuration, it is often used as an analogue for future climate and for climate modeling [*Draut et al*., 2003; *Loutre and Berger*, 2003; *Dickson et al*., 2010]. Furthermore, it has been suggested that increased salt leakage could have intensified the meridional overturning circulation during MIS 11 [*Dickson et al*., 2010], consistent with the better preservation of the salinity (rather than temperature) component of Agulhas leakage as it becomes incorporated into the Atlantic circulation [*Weijer et al*., 2002; *Beal et al*., 2011]. The new data presented here for ODP Site 1087 indicate that salinity (as recorded by negative $\delta D_{alkenone}$ values) is closely linked to the length of interglacials according to benthic $\delta^{18}O$ for at least the last 500 ka. Further work is required to confirm whether this signature is replicated more widely in the Agulhas leakage region and propagated downstream to contribute to AMOC. The SST and $\delta D_{alkenones}$ records from ODP Site1087 demonstrate that a complex relationship exists between signals of early deglacial SST warming in the Southeast Atlantic (and inferred increased Agulhas leakage) and the magnitude or duration of superinterglacials.

4.4. ODP Site 1087 and Impacts on Changing Circulation

The most important proposed impact of Agulhas leakage is on the AMOC. While over shorter time scales both modeling studies [*Biastoch et al*., 2008] and proxy data [*Martínez-Méndez et al*., 2008; *Dickson et al*., 2010; *Marino et al*., 2013; *Koutsodendris et al*., 2014] have shown connections between strengthening of the Agulhas leakage and changes in the AMOC, very little work has been undertaken over multiple glacials and interglacials with the foraminifera analysis at ODP Site 1087 being the one exception [*Caley et al*., 2014]. The new alkenone data presented here for SST and SSS support the proposal of *Caley et al*. [2014] that Agulhas leakage to the Southeast Atlantic has increased overall since 500 ka. The long-term warming from 500 ka to present has only been observed in a few other records besides ODP Site 1087, many of which are in the Benguela upwelling, including ODP Site 1082 [*Etourneau et al*., 2009, 2010; *McClymont et al*., 2013].

Etourneau et al. [2009, 2010] proposed that the warming at ODP Site 1082 reflected a weakening of the Hadley cells through the late Pleistocene; this interpretation is consistent with the overall strengthening of Agulhas leakage that is inferred here from ODP Site 1087 [*Laurian and Drijfhout*, 2011; *Kohfeld et al*., 2013].

At the same time, a number of inorganic δ^{13}C records from benthic foraminifera also show increasing isotope values after 500 ka, especially those records in the Atlantic Ocean [*Raymo et al*., 1997; *Elderfield and Ganssen*, 2000; *Elderfield et al*., 2012; *Bard and Rickaby*, 2009]. Additionally, δ^{13}C records from the Pacific deep waters generally increase after 300 ka [*Mix et al*., 1995]. Therefore, one interpretation for the increasing δ^{13}C values over the last 500 ka is a more vigorous overturning circulation [*Raymo et al*., 1990, 2004; *Bard and Rickaby*, 2009], consistent with the inferred strengthening Agulhas leakage observed at ODP Site 1087 and supported by numerical models and higher-resolution study proxy analyses [*Lutjeharms*, 1981, 2007; *Gordon*, 1985; *de Ruijter et al*., 1999; *Schonten et al*., 2000; *Franzese et al*., 2006b; *Biastoch et al*., 2008; *Laurian and Drijfhout*, 2011]. However, the benthic δ^{13}C records are complex, and alternative interpretations for the North Atlantic sites include local changes in the source deep water, although they may also be linked to changes in AMOC [*Raymo et al*., 2004; *Huybers et al*., 2007]. Furthermore, it is possible that inputs into the overturning circulation only affect the amount of salt and heat in the current and not its strength or speed [*Beal et al*., 2011; *Kohfeld et al*., 2013], so that changing Agulhas leakage may have limited impact on circulation intensity downstream.

5. Conclusions

SSTs, SSS variability, and export production at ODP Site 1087 were reconstructed to investigate changes to the surface waters of the Southeast Atlantic over the last 500 ka. MIS 10 is highlighted as an anomalous glacial stage within the ODP Site 1087 record, marked by pronounced and sustained cooling and high export production. We infer that, at this site, MIS 10 is characterized by an expansion and/or intensification of Benguela upwelling in the southern Benguela region. Through the rest of the record, a consistent pattern of increasing SST and SSS before the onset of deglaciation is observed, interpreted here to indicate an increase in Agulhas leakage associated with glacial-interglacial transitions. However, there is a temporal offset between the (early) increase in SSS and (delayed) increase in SST, although both lead the deglaciation as indicated by benthic δ^{18}O. The new alkenone data at ODP Site 1087 thus show that the process of Agulhas leakage on glacial-interglacial time scales is more complex than a simple and synchronous increase in warm and saline water transport to the Southeast Atlantic and that these two variables can be decoupled. This means that a better understanding of the full nature of the different components of Agulhas leakage, especially SSS, is required to better understand the downstream impacts of the system. This may be particularly important when considering the relationship between the long-term trend of increasing SSTs and SSS toward the present day, suggesting that the overall influence of Agulhas leakage to the Southeast Atlantic has increased through the late Pleistocene, and evidence for an overall intensification of AMOC across the same time interval.

Acknowledgments

This research used samples provided by the Integrated Ocean Drilling Program. Funding for this research was provided by the School of Geography, Politics and Sociology (Newcastle University) by a PhD studentship (B.F.P.). We also thank Catherine Pierre, Jacques Giraudeau, Dick Kroon, Thibaut Caley, and Gema Martinez-Mendez for the provision of data and Aurora Elmore, Rebecca Payne, Andrew Henderson, Richard Pancost, and James Petrick for their constructive comments on an earlier draft of the manuscript. Marcel van der Meer was funded by the Dutch Organisation for Scientific Research (NWO) through a VIDI grant. Finally, we would like to thank anonymous reviewers for their helpful and constructive comments. The data presented in this article are available by e-mail to Benjamin Petrick: benjamin.petrick@ncl.ac.uk

References

Alonso-Garcia, M., F. J. Sierro, and J. A. Flores (2011), Arctic front shifts in the subpolar North Atlantic during the mid-Pleistocene (800-400 ka) and their implications for ocean circulation, *Palaeogeogr. Palaeoclimatol. Palaeoecol.*, *311*(3–4), 268–280, doi:10.1016/j.palaeo.2011.09.004.

Andrews, W. R. H., and D. L. Cram (1969), Combined aerial and shipboard upwelling study in the Benguela Current, *Nature*, *224*(5222), 902–904.

Andrews, W. R. H., and L. Hutchings (1980), Upwelling in the southern Benguela Current, *Prog. Oceanogr.*, *9*(1), 1,IN1,9,IN3,77–8,IN2,76,IN4,81.

Bard, E., and R. E. M. Rickaby (2009), Migration of the subtropical front as a modulator of glacial climate, *Nature*, *460*(7253), 380–393, doi:10.1038/nature08189.

Beal, L. M., W. P. M. De Ruijter, A. Biastoch, and R. Zahn (2011), On the role of the Agulhas system in ocean circulation and climate, *Nature*, *472*(7344), 429–436.
Berger, A., and M. F. Loutre (2002), Climate: An exceptionally long interglacial ahead?, *Science*, *297*(5585), 1287–1288, doi:10.1126/science.1076120.
Biastoch, A., C. W. Boning, and J. R. E. Lutjeharms (2008), Agulhas leakage dynamics affects decadal variability in Atlantic overturning circulation, *Nature*, *456*(7221), 489–492, doi:10.1038/nature07426.
Biastoch, A., C. W. Boning, F. U. Schwarzkopf, and J. R. E. Lutjeharms (2009), Increase in Agulhas leakage due to poleward shift of Southern Hemisphere westerlies, *Nature*, *462*(7272), 495–498.
Boebel, O., R. E. Davis, M. Ollitrault, R. G. Peterson, P. L. Richardson, C. Schmid, and W. Zenk (1999), The intermediate depth circulation of the western South Atlantic, *Geophys. Res. Lett.*, *26*(21), 3329–3332, doi:10.1029/1999GL002355.
Boebel, O., J. Lutjeharms, C. Schmid, W. Zenk, T. Rossby, and C. Barron (2003), The Cape Cauldron: A regime of turbulent inter-ocean exchange, *Deep Sea Res., Part II*, *50*(1), 57–86.
Boudra, D. B., and W. P. M. De Ruijter (1986), The wind-driven circulation of the South Atlantic-Indian Ocean—II. Experiments using a multi-layer numerical model, *Deep Sea Res., Part A*, *33*(4), 447–482.
Brassell, S. C., G. Eglinton, I. T. Marlowe, U. Pflaumann, and M. Sarnthein (1986), Molecular stratigraphy: A new tool for climatic assessment, *Nature*, *320*(6058), 129–133.
Caley, T., et al. (2011), High-latitude obliquity as a dominant forcing in the Agulhas current system, *Clim. Past*, *7*(4), 1285–1296, doi:10.5194/cp-7-1285-2011.
Caley, T., J. Giraudeau, B. Malaize, L. Rossignol, and C. Pierre (2012), Agulhas leakage as a key process in the modes of Quaternary climate changes, *Proc. Natl. Acad. Sci. U.S.A.*, *109*(18), 6835–6839, doi:10.1073/pnas.1115545109.
Caley, T., F. J. C. Peeters, A. Biastoch, L. Rossignol, E. van Sebille, J. Durgadoo, B. Malaizé, J. Giraudeau, K. Arthur, and R. Zahn (2014), Quantitative estimate of the paleo-Agulhas leakage, *Geophys. Res. Lett.*, *41*, 1238–1246, doi:10.1002/2014GL059278.
Chivall, D., D. M'Boule, D. Sinke-Schoen, J. S. Sinninghe Damsté, S. Schouten, and M. T. J. van der Meer (2014), The effects of growth phase and salinity on the hydrogen isotopic composition of alkenones produced by coastal haptophyte algae, *Geochim. Cosmochim. Acta*, *140*, 381–390, doi:10.1016/j.gca.2014.05.043.
Conkright, M. E., R. A. Locarnini, H. E. Garcia, T. D. O'Brien, T. P. Boyer, C. Stephens, and J. I. Antonov (2002), World ocean atlas 2001: Objective analyses, data statistics, and figures, CD-ROM documentation, 17 pp., Natl. Oceanogr. Data Cent., Silver Spring, Md.
Conte, M. H., M.-A. Sicre, C. Rühlemann, J. C. Weber, S. Schulte, D. Schulz-Bull, and T. Blanz (2006), Global temperature calibration of the alkenone unsaturation index (U(37)(K)) in surface waters and comparison with surface sediments, *Geochem. Geophys. Geosyst.*, *7*, Q02005, doi:10.1029/2005GC001054.
Cortese, G., and A. Abelmann (2002), Radiolarian-based paleotemperatures during the last 160 kyr at ODP Site 1089 (Southern Ocean, Atlantic sector), *Palaeogeogr. Palaeoclimatol. Palaeoecol.*, *182*(3-4), 259–286, doi:10.1016/s0031-0182(01)00499-0.
Cortese, G., A. Abelmann, and R. Gersonde (2004), A glacial warm water anomaly in the subantarctic Atlantic Ocean, near the Agulhas retroflection, *Earth Planet. Sci. Lett.*, *222*(3–4), 767–778.
Cortese, G., A. Abelmann, and R. Gersonde (2007), The last five glacial-interglacial transitions: A high-resolution 450,000-year record from the subantarctic Atlantic, *Paleoceanography*, *22*, PA4203, doi:10.1029/2007PA001457.
De Abreu, C., F. F. Abrantes, N. J. Shackleton, P. C. Tzedakis, J. F. McManus, D. W. Oppo, and M. A. Hall (2005), Ocean climate variability in the eastern North Atlantic during interglacial marine isotope stage 11: A partial analogue to the Holocene?, *Paleoceanography*, *20*, PA3009, doi:10.1029/2004PA001091.
De Boer, A. M., R. M. Graham, M. D. Thomas, and K. E. Kohfeld (2013), The control of the Southern Hemisphere westerlies on the position of the Subtropical Front, *J. Geophys. Res. Oceans*, *118*, 5669–5675, doi:10.1002/jgrc.20407.
De Deckker, P., M. Moros, K. Perner, and E. Jansen (2012), Influence of the tropics and southern westerlies on glacial interhemispheric asymmetry, *Nat. Geosci.*, *5*(4), 266–269, doi:10.1038/ngeo1431.
De Ruijter, W. P. M., and D. B. Boudra (1985), The wind-driven circulation in the South Atlantic-Indian Ocean—I. Numerical experiments in a one-layer model, *Deep Sea Res., Part A*, *32*(5), 557–574.
De Ruijter, W. P. M., A. Biastoch, S. S. Drijfhout, J. R. E. Lutjeharms, R. P. Matano, T. Pichevin, P. J. van Leeuwen, and W. Weijer (1999), Indian-Atlantic interocean exchange: Dynamics, estimation and impact, *J. Geophys. Res.*, *104*(C9), 20,885–20,910, doi:10.1029/1998JC900099.
De Schepper, S., M. J. Head, and J. Groeneveld (2009), North Atlantic Current variability through marine isotope stage M2 (circa 3.3 Ma) during the mid-Pliocene, *Paleoceanography*, *24*, PA4206, doi:10.1029/2008PA001725.
De Vernal, A., and C. Hillaire-Marcel (2000), Sea-ice cover, sea-surface salinity and halo-thermocline structure of the northwest North Atlantic: Modern versus full glacial conditions, *Quat. Sci. Rev.*, *19*(1–5), 65–85, doi:10.1016/S0277-3791(99)00055-4.
De Vernal, A., et al. (2005), Reconstruction of sea-surface conditions at middle to high latitudes of the Northern Hemisphere during the Last Glacial Maximum (LGM) based on dinoflagellate cyst assemblages, *Quat. Sci. Rev.*, *24*(7–9), 897–924, doi:10.1016/j.quascirev.2004.06.014.
DeConto, R., D. Pollard, and D. Harwood (2007), Sea ice feedback and Cenozoic evolution of Antarctic climate and ice sheets, *Paleoceanography*, *22*, PA3214, doi:10.1029/2006PA001350.
Dickson, A. J., C. J. Beer, C. Dempsey, M. A. Maslin, J. A. Bendle, E. L. McClymont, and R. D. Pancost (2009), Oceanic forcing of the marine isotope stage 11 interglacial, *Nat. Geosci.*, *2*(6), 427–432, doi:10.1038/ngeo527.
Dickson, A. J., M. J. Leng, M. A. Maslin, H. J. Sloane, J. Green, J. A. Bendle, E. L. McClymont, and R. D. Pancost (2010), Atlantic overturning circulation and Agulhas leakage influences on Southeast Atlantic upper ocean hydrography during marine isotope stage 11, *Paleoceanography*, *25*, PA3208, doi:10.1029/2009PA001830.
Draut, A. E., M. E. Raymo, J. F. McManus, and D. W. Oppo (2003), Climate stability during the Pliocene warm period, *Paleoceanography*, *18*(4), 1078, doi:10.1029/2003PA000889.
Elderfield, H., and G. Ganssen (2000), Past temperature and delta180 of surface ocean waters inferred from foraminiferal Mg/Ca ratios, *Nature*, *405*(6785), 442–445.
Elderfield, H., P. Ferretti, M. Greaves, S. Crowhurst, I. N. McCave, D. Hodell, and A. M. Piotrowski (2012), Evolution of ocean temperature and ice volume through the mid-Pleistocene climate transition, *Science*, *337*(6095), 704–709, doi:10.1126/science.1221294.
Emeis, K.-C., D. M. Anderson, H. Doose, D. Kroon, and D. Schulz-Bull (1995), Sea-surface temperatures and the history of monsoon upwelling in the northwest Arabian sea during the last 500,000 years, *Quat. Res.*, *43*(3), 355–361, doi:10.1006/qres.1995.1041.
EPICA (2004), Eight glacial cycles from an Antarctic ice core, *Nature*, *429*(6992), 623–628, doi:10.1038/nature02599.
Etourneau, J., P. Martinez, T. Blanz, and R. Schneider (2009), Pliocene-Pleistocene variability of upwelling activity, productivity, and nutrient cycling in the Benguela region, *Geology*, *37*(10), 871–874, doi:10.1130/g25733a.1.
Etourneau, J., R. Schneider, T. Blanz, and P. Martinez (2010), Intensification of the Walker and Hadley atmospheric circulations during the Pliocene-Pleistocene climate transition, *Earth Planet. Sci. Lett.*, *297*(1–2), 103–110.

Franzese, A. M., S. R. Hemming, S. L. Goldstein, and R. F. Anderson (2006a), Reduced Agulhas leakage during the Last Glacial Maximum inferred from an integrated provenance and flux study, *Earth Planet. Sci. Lett.*, *250*(1–2), 72–88, doi:10.1016/j.epsl.2006.07.002.
Franzese, A. M., S. R. Hemming, S. L. Goldstein, and R. F. Anderson (2006b), Reduced Agulhas leakage during the Last Glacial Maximum inferred from an integrated provenance and flux study, *Earth Planet. Sci. Lett.*, *250*(1–2), 72–88, doi:10.1016/j.epsl.2006.07.002.
Garzoli, S. L., and R. Matano (2011), The South Atlantic and the Atlantic meridional overturning circulation, *Deep Sea Res., Part II*, *58*(17–18), 1837–1847.
Giraudeau, J., C. Pierre, and L. Herve (2001), A late Quarternary, high-resolution record of planktonic foraminiferal species distribution in the southern Benguela region: Site 1087, in *Proceedings of the Ocean Drilling Program, Sci. Results*, vol. 175, edited by G. Wefer, W. H. Berger, and C. Richter, pp. 1–26, Ocean Drill. Program, College Station, Tex., doi:10.2973/odp.proc.sr.175.225.2001.
Gordon, A. L. (1985), Indian-Atlantic transfer of thermocline water at the Agulhas retroflection, *Science*, *227*(4690), 1030–1033, doi:10.1126/science.227.4690.1030.
Gordon, A. L., J. R. E. Lutjeharms, and M. L. Gründlingh (1987), Stratification and circulation at the Agulhas retroflection, *Deep Sea Res., Part A*, *34*(4), 565–599.
Harris, P. G., M. Zhao, A. Rosell-Mele, R. Tiedemann, M. Sarnthein, and J. R. Maxwell (1996), Chlorin accumulation rate as a proxy for Quaternary marine primary productivity, *Nature*, *383*(6595), 63–65.
Hutchings, L., et al. (2009), The Benguela Current: An ecosystem of four components, *Prog. Oceanogr.*, *83*(1–4), 15–32.
Huybers, P., G. Gebbie, and O. Marchal (2007), Can paleoceanographic tracers constrain meridional circulation rates?, *J. Phys. Oceanogr.*, *37*(2), 394–407, doi:10.1175/JPO3018.1.
Kasper, S., M. T. J. van der Meer, A. Mets, R. Zahn, J. S. Sinninghe Damsté, and S. Schouten (2014), Salinity changes in the Agulhas leakage area recorded by stable hydrogen isotopes of C_{37} alkenones during Termination I and II, *Clim. Past*, *10*(1), 251–260, doi:10.5194/cp-10-251-2014.
Kasper, S., M. T. J. van der Meer, I. S. Castañeda, R. Tjallingii, G.-J. A. Brummer, J. S. Sinninghe Damsté, and S. Schouten (2015), Testing the alkenone D/H ratio as a paleo indicator of sea surface salinity in a coastal ocean margin (Mozambique Channel), *Org. Geochem.*, *78*, 62–68, doi:10.1016/j.orggeochem.2014.10.011.
Knorr, G., and G. Lohmann (2003), Southern Ocean origin for the resumption of Atlantic thermohaline circulation during deglaciation, *Nature*, *424*(6948), 532–536, doi:10.1038/nature01855.
Kohfeld, K. E., R. M. Graham, A. M. de Boer, L. C. Sime, E. W. Wolff, C. Le Quéré, and L. Bopp (2013), Southern Hemisphere westerly wind changes during the Last Glacial Maximum: Paleo-data synthesis, *Quat. Sci. Rev.*, *68*, 76–95, doi:10.1016/j.quascirev.2013.01.017.
Kornilova, O., and A. Rosell-Mele (2003), Application of microwave-assisted extraction to the analysis of biomarker climate proxies in marine sediments, *Org. Geochem.*, *34*(11), 1517–1523, doi:10.1016/s0146-6380(03)00155-4.
Koutsodendris, A., J. Pross, and R. Zahn (2014), Exceptional Agulhas leakage prolonged interglacial warmth during MIS 11c in Europe, *Paleoceanography*, *29*, 1062–1071, doi:10.1002/2014PA002665.
Laurian, A., and S. S. Drijfhout (2011), Response of the South Atlantic circulation to an abrupt collapse of the Atlantic meridional overturning circulation, *Clim. Dyn.*, *37*(3–4), 521–530, doi:10.1007/s00382-010-0890-3.
Leduc, G., C. T. Herbert, T. Blanz, P. Martinez, and R. Schneider (2010), Contrasting evolution of sea surface temperature in the Benguela upwelling system under natural and anthropogenic climate forcings, *Geophys. Res. Lett.*, *37*, L20705, doi:10.1029/2010GL044353.
Lee, K. E., J.-H. Kim, I. Wilke, P. Helmke, and S. Schouten (2008), A study of the alkenone, TEX86, and planktonic foraminifera in the Benguela upwelling system: Implications for past sea surface temperature estimates, *Geochem. Geophys. Geosyst.*, *9*, Q10019, doi:10.1029/2008GC002056.
Lisiecki, L. E., and M. E. Raymo (2005), A Pliocene-Pleistocene stack of 57 globally distributed benthic delta O-18 records, *Paleoceanography*, *20*, PA1003, doi:10.1029/2004PA001071.
Lisiecki, L. E., and M. E. Raymo (2007), Plio-Pleistocene climate evolution: Trends and transitions in glacial cycle dynamics, *Quat. Sci. Rev.*, *26*(1–2), 56–69, doi:10.1016/j.quascirev.2006.09.005.
Loutre, M. F., and A. Berger (2003), Marine isotope stage 11 as an analogue for the present interglacial, *Global Planet. Change*, *36*(3), 209–217.
Lutjeharms, J. R. E. (1981), Spatial scales and intensities of circulation in the ocean areas adjacent to South Africa, *Deep Sea Res., Part A*, *28*(11), 1289–1302.
Lutjeharms, J. R. E. (1994), The exchange of water between the South Indian and South Atlantic Oceans, in *Symposium on the South Atlantic: Present and Past Circulation*, edited by G. Wefer et al., pp. 125–162, Springer, Berlin.
Lutjeharms, J. R. E. (2007), Three decades of research on the greater Agulhas Current, *Ocean Sci.*, *3*(1), 129–147.
Lutjeharms, J. R. E., and A. L. Gordon (1987), Shedding of an Agulhas ring observed at sea, *Nature*, *325*(6100), 138–140.
Lutjeharms, J. R. E., H. S. John, K. T. Karl, and A. T. Steve (2001), Agulhas Current, in *Encyclopedia of Ocean Sciences*, pp. 128–137, Academic Press, Oxford.
M'boule, D., D. Chivall, D. Sinke-Schoen, J. S. Sinninghe Damsté, S. Schouten, and M. T. J. van der Meer (2014), Salinity dependent hydrogen isotope fractionation in alkenones produced by coastal and open ocean haptophyte algae, *Geochim. Cosmochim. Acta*, *130*, 126–135, doi:10.1016/j.gca.2014.01.029.
Marino, G., R. Zahn, M. Ziegler, C. Purcell, G. Knorr, I. R. Hall, P. Ziveri, and H. Elderfield (2013), Agulhas salt-leakage oscillations during abrupt climate changes of the late Pleistocene, *Paleoceanography*, *28*, 599–606, doi:10.1002/palo.20038.
Marlow, J. R., C. B. Lange, G. Wefer, and A. Rosell-Mele (2000), Upwelling intensification as part of the Pliocene-Pleistocene climate transition, *Science*, *290*(5500), 2288–2291.
Marret, F., and K. A. F. Zonneveld (2003), Atlas of modern organic-walled dinoflagellate cyst distribution, *Rev. Palaeobot. Palynol.*, *125*(1–2), 1–200, doi:10.1016/s0034-6667(02)00229-4.
Marret, F., J. Scourse, H. Kennedy, E. Ufkes, and J. H. F. Jansen (2008), Marine production in the Congo-influenced SE Atlantic over the past 30,000 years: A novel dinoflagellate-cyst based transfer function approach, *Mar. Micropaleontol.*, *68*(1–2), 198–222, doi:10.1016/j.marmicro.2008.01.004.
Martinez-Garcia, A., A. Rosell-Mele, S. L. Jaccard, W. Geibert, D. M. Sigman, and G. H. Haug (2011), Southern Ocean dust-climate coupling over the past four million years, *Nature*, *476*(7360), 312–315.
Martínez-Méndez, G., R. Zahn, I. R. Hall, L. D. Pena, and I. Cacho (2008), 345,000-year-long multi-proxy records off South Africa document variable contributions of northern versus southern component water to the deep South Atlantic, *Earth Planet. Sci. Lett.*, *267*(1–2), 309–321.
Martínez-Méndez, G., R. Zahn, I. R. Hall, F. J. C. Peeters, L. D. Pena, I. Cacho, and C. Negre (2010), Contrasting multiproxy reconstructions of surface ocean hydrography in the Agulhas Corridor and implications for the Agulhas leakage during the last 345,000 years, *Paleoceanography*, *25*, PA4227, doi:10.1029/2009PA001879.
Masson-Delmotte, V., et al. (2010), EPICA Dome C record of glacial and interglacial intensities, *Quat. Sci. Rev.*, *29*(1–2), 113–128.

McClymont, E. L., A. Rosell-Mele, J. Giraudeau, C. Pierre, and J. M. Lloyd (2005), Alkenone and coccolith records of the mid-Pleistocene in the south-east Atlantic: Implications for the U-37(K) index and South African climate, *Quat. Sci. Rev.*, *24*(14–15), 1559–1572, doi:10.1016/j.quascirev.2004.06.024.

McClymont, E. L., S. M. Sosdianb, and Y. Rosenthalb (2013), Pleistocene sea-surface temperature evolution: Early cooling, delayed glacial intensification, and implications for the mid-Pleistocene climate transition, *Earth Sci. Rev.*, *123*, 173–193.

Mix, A. C., J. Le, and N. J. Shackleton (1995), Benthic foraminiferal stable isotope stratigraphy of Site 846: 0–1.8 Ma, *Proc. Ocean Drill. Program: Sci. Results*, *138*, 839–854.

Müller, P. J., M. Cepek, G. Ruhland, and R. R. Schneider (1997), Alkenone and coccolithophorid species changes in late Quaternary sediments from the Walvis Ridge: Implications for the alkenone paleotemperature method, *Palaeogeogr. Palaeoclimatol. Palaeoecol.*, *135*(1–4), 71–96.

Müller, P. J., G. Kirst, G. Ruhland, I. von Storch, and A. Rosell-Mele (1998), Calibration of the alkenone paleotemperature index U-37(K') based on core-tops from the eastern South Atlantic and the global ocean (60°N–60°S), *Geochim. Cosmochim. Acta*, *62*(10), 1757–1772.

Olson, D. B., and R. H. Evans (1986), Rings of the Agulhas Current, *Deep Sea Res., Part A*, *33*(1), 27–42.

Paillard, D., L. Labeyrie, and P. Yiou (1996), Macintosh program performs time-series analysis, *Eos, Trans. Am. Geophys. Union*, *77*, 379.

Peeters, F. J. C., R. Acheson, G.-J. A. Brummer, W. P. M. de Ruijter, R. R. Schneider, G. M. Ganssen, E. Ufkes, and D. Kroon (2004), Vigorous exchange between the Indian and Atlantic Oceans at the end of the past five glacial periods, *Nature*, *430*(7000), 661–665.

Pelejero, C., E. Calvo, T. T. Barrows, G. A. Logan, and P. De Deckker (2006), South Tasman Sea alkenone palaeothermometry over the last four glacial/interglacial cycles, *Mar. Geol.*, *230*(1–2), 73–86, doi:10.1016/j.margeo.2006.04.004.

Penven, P., J. R. E. Lutjeharms, P. Marchesiello, C. Roy, and S. J. Weeks (2001), Generation of cyclonic eddies by the Agulhas Current in the lee of the Agulhas Bank, *Geophys. Res. Lett.*, *28*(6), 1055–1058, doi:10.1029/2000GL011760.

Petrick, B., E. L. McClymont, S. Felder, G. Rueda, M. J. Leng, and A. Rosell-Melé (2015), Late Pliocene upwelling in the southern Benguela region, *Palaeogeogr. Palaeoclimatol. Palaeoecol.*, doi:10.1016/j.palaeo.2015.03.042.

Pierre, C., J. F. Saliege, M. J. Urrutiaguer, and J. Giraudeau (2001), Stable isotope record of the last 500 k.y. at Site 1087 (southern Cape Basin), in *Proceedings of the Ocean Drilling Program, Sci. Results*, vol. 175, edited by G. Wefer, W. H. Berger, and C. Richter, pp. 1–22, Ocean Drill. Program, College Station, Tex.

Pollard, D., and R. M. DeConto (2009), Modelling West Antarctic ice sheet growth and collapse through the past five million years, *Nature*, *458*(7236), 329–332.

Prahl, F. G., and S. G. Wakeham (1987), Calibration of unsaturation patterns in long-chain ketone compositions for paleotemperature assessment, *Nature*, *330*(6146), 367–369.

Prahl, F. G., L. A. Muehlhausen, and D. L. Zahnle (1988), Further evaluation of long-chain alkenones as indicators of paleoceanographic conditions, *Geochim. Cosmochim. Acta*, *52*(9), 2303–2310.

Prahl, F. G., G. J. de Lange, M. Lyle, and M. A. Sparrow (1989), Post-depositional stability of long-chain alkenones under contrasting redox conditions, *Nature*, *341*(6241), 434–437.

Rau, A. J., J. Rogers, J. R. E. Lutjeharms, J. Giraudeau, J. A. Lee-Thorp, M. T. Chen, and C. Waelbroeck (2002), A 450-kyr record of hydrological conditions on the western Agulhas Bank Slope, south of Africa, *Mar. Geol.*, *180*(1–4), 183–201.

Raymo, M. E., W. F. Ruddiman, N. J. Shackleton, and D. W. Oppo (1990), Evolution of Atlantic-Pacific d13C gradients over the last 2.5 m.y, *Earth Planet. Sci. Lett.*, *97*(3–4), 353–368, doi:10.1016/0012-821X(90)90051-X.

Raymo, M. E., D. W. Oppo, and W. Curry (1997), The mid-Pleistocene climate transition: A deep sea carbon isotopic perspective, *Paleoceanography*, *12*(4), 546–559, doi:10.1029/97PA01019.

Raymo, M. E., D. W. Oppo, B. P. Flower, D. A. Hodell, J. F. McManus, K. A. Venz, K. F. Kleiven, and K. McIntyre (2004), Stability of North Atlantic water masses in face of pronounced climate variability during the Pleistocene, *Paleoceanography*, *19*, PA2008, doi:10.1029/2003PA000921.

Rosell-Melé, A., M. A. Maslin, J. R. Maxwell, and P. Schaeffer (1997), Biomarker evidence for "Heinrich" events, *Geochim. Cosmochim. Acta*, *61*(8), 1671–1678, doi:10.1016/S0016-7037(97)00046-X.

Rosell-Melé, A., A. Martínez-Garcia, and E. L. McClymont (2014), Persistent warmth across the Benguela upwelling system during the Pliocene epoch, *Earth Planet. Sci. Lett.*, *386*, 10–20, doi:10.1016/j.epsl.2013.10.041.

Schonten, M. W., W. P. M. de Ruijter, P. J. van Leeuwen, and J. R. E. Lutjeharms (2000), Translation, decay and splitting of Agulhas rings in the southeastern Atlantic Ocean, *J. Geophys. Res.*, *105*(C9), 21,913–21,925, doi:10.1029/1999JC000046.

Schouten, S., J. Ossebaar, K. Schreiber, M. V. M. Kienhuis, G. Langer, A. Benthien, and J. Bijma (2006), The effect of temperature, salinity and growth rate on the stable hydrogen isotopic composition of long chain alkenones produced by *Emiliania huxleyi* and *Gephyrocapsa oceanica*, *Biogeosciences*, *3*(1), 113–119, doi:10.5194/bg-3-113-2006.

Scussolini, P., G. Marino, G.-J. A. Brummer, and F. J. C. Peeters (2015), Saline Indian Ocean waters invaded the South Atlantic thermocline during glacial termination II, *Geology*, *43*(2), 139–142, doi:10.1130/G36238.1.

Sexton, P. F., and R. D. Norris (2011), High latitude regulation of low latitude thermocline ventilation and planktic foraminifer populations across glacial-interglacial cycles, *Earth Planet. Sci. Lett.*, *311*(1–2), 69–81, doi:10.1016/j.epsl.2011.08.044.

Shipboard Scientific Party (1998), Introduction: Background, scientific objectives, and principal results for Leg 175 (Benguela Current and Angola-Benguela upwelling systems), in *Proceedings of the Ocean Drilling Program, Initial Rep.*, vol. 175, edited by G. Wefer et al., pp. 7–25, Ocean Drill. Program, College Station, Tex.

Szymczak-Zyla, M., G. Kowalewska, and J. W. Louda (2011), Chlorophyll-*a* and derivatives in recent sediments as indicators of productivity and depositional conditions, *Mar. Chem.*, *125*(1–4), 39–48.

Turney, C., R. Jones, H. Rashid, F. O. Otieno, and M. K. Konfirst (2011), Comments on "Does the Agulhas Current amplify global temperatures during super-interglacials?", *J. Quat. Sci.*, *26*(8), 866–869, doi:10.1002/jqs.1550.

Turney, C. S., and R. T. Jones (2010), Does the Agulhas Current amplify global temperatures during super-interglacials?, *J. Quat. Sci.*, *25*(6), 839–843, doi:10.1002/jqs.1423.

Ufkes, E., and D. Kroon (2012), Sensitivity of south-east Atlantic planktonic foraminifera to mid-Pleistocene climate change, *Palaeontology*, *55*, 183–204, doi:10.1111/j.1475-4983.2011.01119.x.

Ufkes, E., J. H. F. Jansen, and R. R. Schneider (2000), Anomalous occurrences of Neogloboquadrina pachyderma (left) in a 420-ky upwelling record from Walvis Ridge (SE Atlantic), *Mar. Micropaleontol.*, *40*(1–2), 23–42.

Van der Meer, M. T. J., M. Baas, W. I. C. Rijpstra, G. Marino, E. J. Rohling, J. S. Sinninghe Damsté, and S. Schouten (2007), Hydrogen isotopic compositions of long-chain alkenones record freshwater flooding of the Eastern Mediterranean at the onset of sapropel deposition, *Earth Planet. Sci. Lett.*, *262*, 594–600.

Van der Meer, M. T. J., F. Sangiorgi, M. Baas, H. Brinkhuis, J. S. Sinninghe Damsté, and S. Schouten (2008), Molecular isotopic and dinoflagellate evidence for Late Holocene freshening of the Black Sea, *Earth Planet. Sci. Lett.*, *267*, 426–434.

Van der Meer, M. T. J., A. Benthien, J. Bijma, S. Schouten, and J. S. Sinninghe Damsté (2013), Alkenone distribution impacts the hydrogen isotopic composition of the C37:2 and C37:3 alkan-2-ones in Emiliania huxleyi, *Geochim. Cosmochim. Acta*, *111*, 162–166, doi:10.1016/j.gca.2012.10.041.

Volkman, J. K., G. Eglinton, E. D. S. Corner, and T. E. V. Forsberg (1980), Long-chain alkenes and alkenones in the marine coccolithophorid Emiliania huxleyi, *Phytochemistry*, *19*(12), 2619–2622.

Weijer, W., W. P. M. de Ruijter, H. A. Dijkstra, and P. J. van Leeuwen (1999), Impact of interbasin exchange on the Atlantic overturning circulation, *J. Phys. Oceanogr.*, *29*(9), 2266–2284.

Weijer, W., W. P. M. De Ruijter, A. Sterl, and S. S. Drijfhout (2002), Response of the Atlantic overturning circulation to South Atlantic sources of buoyancy, *Global Planet. Change*, *34*(3–4), 293–311.

Zonneveld, K. A. F., R. P. Hoek, H. Brinkhuis, and H. Willems (2001), Geographical distributions of organic-walled dinoflagellate cysts in surficial sediments of the Benguela upwelling region and their relationship to upper ocean conditions, *Prog. Oceanogr.*, *48*(1), 25–72, doi:10.1016/s0079-6611(00)00047-1.